ADVANCED FUNCTIONAL MATERIALS
www.afm-journal.de

Optical Gating of Photosensitive Synthetic Ion Channels

Mubarak Ali, Saima Nasir, Patricio Ramirez, Ishtiaq Ahmed, Quoc Hung Nguyen, Ljiljana Fruk, Salvador Mafe, and Wolfgang Ensinger*

4-oxo-4-(pyren-4-ylmethoxy) butanoic acid is used as a photolabile protecting group to show the optical gating of nanofluidic devices based on synthetic ion channels. The inner surface of the channels is decorated with monolayers of photolabile hydrophobic molecules that can be removed by irradiation, which leads to the generation of hydrophilic groups. This process can be exploited in the UV-light-triggered permselective transport of ionic species in aqueous solution through the channels. The optical gating of a single conical nanochannel and multichannel polymeric membranes is characterised experimentally and theoretically by means of current–voltage and selective permeation measurements, respectively. It is anticipated that the integration of nanostructures into multifunctional devices is feasible and can readily find applications in light-induced controlled release, sensing, and information processing.

1. Introduction

The miniaturisation of fluidic devices that may respond to external triggering is crucial to mimic and exploit the functionality of biological ion channels in health sciences and biotechnology.[1,2] In nature, ion channels regulate the flow of permeants across the cell membrane, allowing physiological functions such as energy storage and signal transduction.[3] Natural ion channels and pores such as α-hemolysin provide structures whose interfacial chemistry can be controlled with high precision.[4] However, these nanostructures are not suitable for practical applications due to their fragility and the sensitivity of the embedding lipid bilayer to external parameters such as pH, temperature, and salt concentration. Synthetic nanochannels show some advantages over their biological counterparts such as stability, tunable channel diameter and shape, possibility of integration into nanofluidic devices, and tailored surface properties.[5,6] Furthermore, these nanochannels exhibit transport properties similar to those of biological ion channels, such as current rectification, voltage-dependent current gating, and permselectivity to ionic species.[7–10] In particular, current rectification in conical nanochannels and nanopipettes occurs due to the combined effect of the surface charge and the conical geometry under an applied voltage.[11–13]

Several approaches have been pursued to achieve active control over ion transport in nanoconfined geometries. To this end, the channel surface was decorated with a variety of chemical functionalities that responded to external stimuli such as ions in solution,[14] biomolecules,[15–18] light,[19,20] the solution pH,[21–23] temperature[24] and combinations of both pH and temperature.[25] The design of nanochannels sensitive to ultraviolet (UV) light still constitutes a challenge for current techniques. Unlike a chemical stimulus, UV light is noninvasive and the whole process can easily be tuned by manipulating the light wavelength. Moreover, UV light can be used to induce a wide range of photochemical changes, e.g., triggering molecular rearrangements and leading to the cleavage of chemical bonds.[26]

Numerous photolabile protecting groups (PPGs) have been reported, which are based on different mechanisms involving the excitation of chromophores.[27–29] PPGs have been widely used in organic synthesis,[30] for protecting carbohydrates,[31] in biochemistry (e.g., as "caged compounds"),[32] and in solid phase and combinatorial synthesis.[33,34] The most interesting feature of PPGs is that they can be cleaved upon exposure to long UV wavelength (UV_{365}) without causing any damage to the rest of the molecule directly attached to the substrate. Photoremovable protecting molecules have also been successfully employed in the polymer backbone and self-assembled monolayers to control the surface wettability as well as in controlled release processes.[35–39] Seminal work by Moore and co-workers involved the design and fabrication of microfluidic devices to regulate liquid flow inside the microchannels modified with photocleavable self-assembled monolayers through UV light irradiation.[40]

Here, we describe a novel technique in which photoremovable protecting molecules were used to construct photosensitive

Dr. M. Ali, S. Nasir, Q. H. Nguyen, Prof. W. Ensinger
Department of Material- and Geo-Sciences
Technische Universität Darmstadt
Petersenstrasse 23, D-64287 Darmstadt, Germany
E-mail: m.ali@gsi.de
Dr. M. Ali, S. Nasir, Q. H. Nguyen, Prof. W. Ensinger
Materials Research Department
GSI Helmholtzzentrum für Schwerionenforschung
Planckstrasse 1, D-64291, Darmstadt, Germany
Prof. P. Ramirez
Dept. de Física Aplicada
Universitat Politécnica de València
E-46022 Valencia, Spain
Dr. I. Ahmed, Dr. Lj. Fruk
Karlsruher Institute of Technology
DFG-Center for Functional Nanostructures
Wolfgang-Gaede-Strasse 1, D-76131 Karlsruhe, Germany
Prof. S. Mafe
Dept. de Física de la Terra i Termodinàmica
Universitat de València
E-46100 Burjassot, Spain

DOI: 10.1002/adfm.201102146

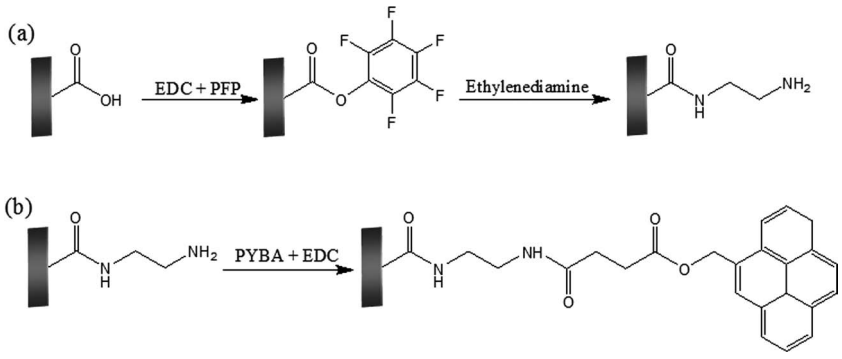

Scheme 1. Scheme of the chemical functionalisation of the inner nanochannel surface.

nanofluidic devices based on synthetic ion channels. For this purpose, the inner walls of the nanochannels are decorated with monolayers of photolabile protecting molecules. Subsequently, the targeted hydrophobic PPGs are removed by using UV light as an external stimulus, leading to the generation of hydrophilic groups that are responsible for the permselective transport of ionic and molecular species through the channels. First, we demonstrate experimentally and theoretically the UV-light-operated single conical nanochannel in a polymer membrane. Second, we integrate a collection of nanochannels in a polymeric membrane to obtain a multifunctional nanofluidic device. We show that optical gating allows the permselective transport of charged species through the membrane nanochannels. Potential applications of the single-nanochannel and the multichannel membranes are light-induced controlled release, sensing, and information processing. In particular, most experimental systems proposed previously are based on chemical signals as inputs and optical (e.g., fluorescence) signals as outputs. The system characterised here could be employed with optical and electrical signals as the inputs and electrical and chemical signal as the outputs.

2. Results and Discussion

Ion track-etched polyethylene terephthalate (PET) membranes containing a single conical nanochannel and cylindrical nanochannel arrays (5×10^8 channels cm^{-2}) were used for the fabrication of the photosensitive nanofluidic devices. During the track-etching process, carboxyl (–COOH) groups were generated on the surface and the inner channel walls.[41] These moieties served as starting points for the introduction of other responsive chemical functionalities onto the channel surface. The immobilisation of PPGs onto the inner channel walls was accomplished in a two-step process (**Scheme 1**),[42] as described in the Experimental Section.

2.1. Single Conical Nanochannels

For the case of a single conical nanochannel, the success of surface modification reactions was corroborated by measuring the current–voltage (*I–V*) characteristics,[16,22,43] which are dictated by the electrostatic interaction of the charged channel surface with the mobile ions in an electrolyte solution.

Figure 1a shows the *I–V* curves prior to and after ethylenediamine (EDA) functionalisation. The recordings were obtained under symmetric electrolyte conditions using a 0.1 M KCl solution prepared in a 10 mM phosphate buffer (pH = 6.0). The current rectification of the single conical nanochannel is due to the surface charge and polarity.[8,11–13] Before modification, the nanochannel is cation selective and thus rectifies the cation flux. The preferential direction of the flux is from the narrow cone opening to the wide opening because of the negative $–COO^-$ groups.[44] After amidation, the nanochannel surface charge was switched from negative to positive, resulting in an anionic selectivity and the concomitant inversion in the rectification characteristics.[17,42,45]

Figure 1b shows the *I–V* curves of the same conical nanochannel, modified now with monolayers of photolabile PYBA molecules, before and after UV_{365}-light irradiation. As expected, immobilisation of 4-oxo-4-(pyren-4-ylmethoxy) butanoic acid (PYBA) resulted in the loss of channel surface charge due to the presence of uncharged terminal pyrene moieties. Eventually, the PYBA-modified channel behaved like an ohmic resistor (the net surface charge on the channel walls was zero). Upon UV_{365}-light irradiation of the PYBA-modified channel, the ester bond adjoining the pyrene chromophore was cleaved,[37,38] resulting in the generation of –COOH functionalities on the channel surface (**Figure 2**). Under our experimental conditions, the exposed carboxylate groups are ionised ($–COO^-$),[44] which restores the cation-selective behaviour of the channel. This reveals that upon UV-light irradiation the inner environment of the nanochannel was switched from a hydrophobic, nonconducting (off) state to a hydrophilic, conducting (on) state (Figure 2). Thus, the UV-light-induced change in the surface charge modulates the permselective behaviour of the channel: the *I–V* curve shows an eight-fold increase in the rectified ionic current (from 100 to 800 pA approximately; see Figure 1b) after UV irradiation. Moreover, the *I–V* curves show a significant recovery of most of the protected carboxyl groups (compare the NH_3^+ curve at $V < 0$ of Figure 1a with the PYBA curve at $V > 0$ after irradiation of Figure 1b.) Light-controlled modulation provides then a feasible tool to externally tune the electrical behaviour of the nanochannel by exploiting the interactions between the charged inner walls and the mobile ionic species in solution.

The experimental results of Figure 1a and b can be described theoretically in terms of a continuous model based on the Poisson and Nernst–Planck (PNP) equations[12]

$$\nabla^2\phi = \frac{F}{\varepsilon}\left(c_{Cl^-} - c_{K^+}\right) \quad (1)$$

$$\nabla \cdot \vec{J}_i = -\nabla \cdot \left[D_i \left(\nabla c_i + z_i c_i \frac{F}{RT} \nabla\phi \right) \right] = 0, \; i = K^+, \; Cl^- \quad (2)$$

where $\vec{J}_i$, c_i, D_i and z_i are the flux, the local concentration, the diffusion coefficient and the charge number of ion i ($i = K^+$ and Cl^-), with ϕ and ε the local electric potential and the dielectric permittivity of the solution within the pore, respectively. F is the Faraday constant, R is the gas constant, and T is the temperature.

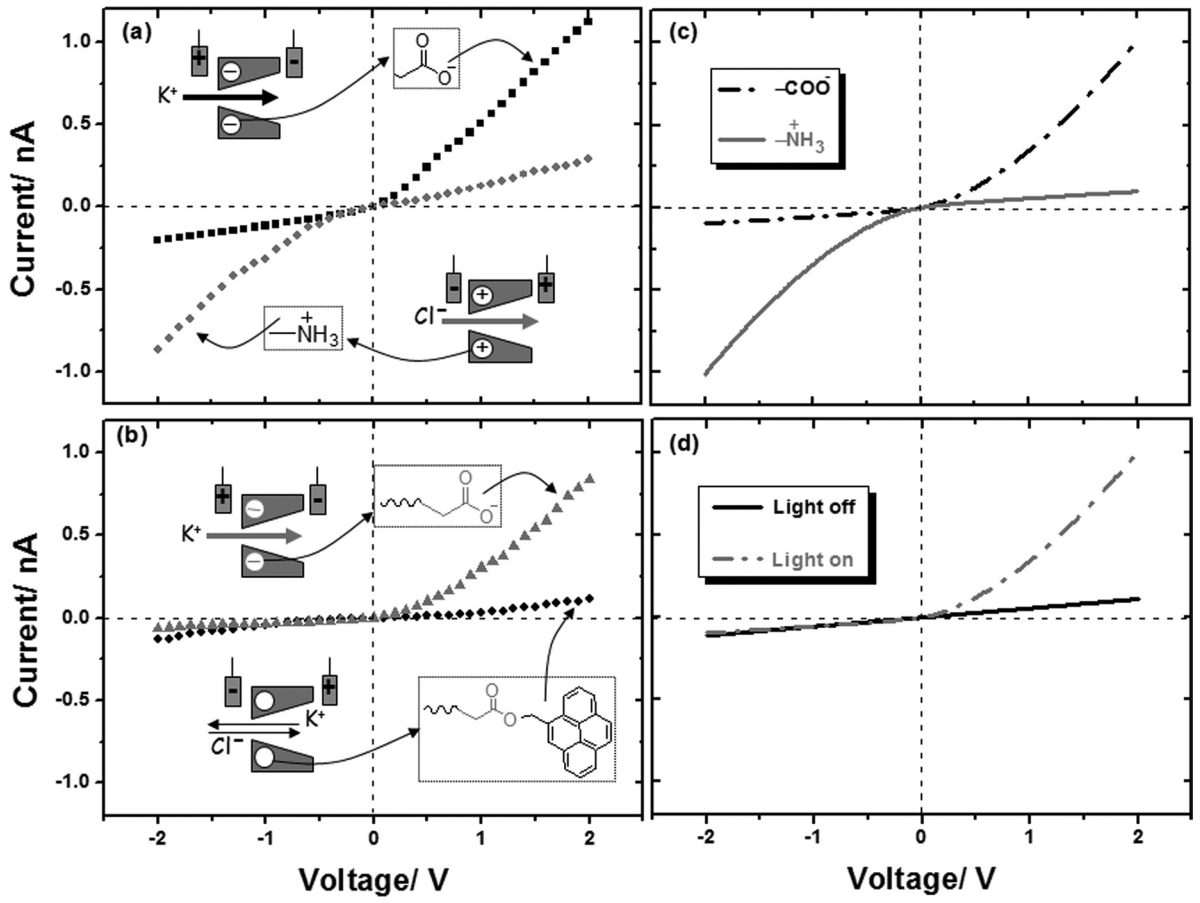

Figure 1. a) *I–V* characteristics of single conical nanochannels bearing ionised carboxyl and amine groups in a 0.1 M KCl (pH = 6.0) aqueous solution. b) *I–V* characteristics of the same nanochannel modified with photosensitive PYBA molecules before and after UV light irradiation. c,d) *I–V* theoretical curves corresponding to the experimental curves (a) and (b) respectively. The approximate radii are a_B = 140 nm for the channel base and a_T = 2 nm for the channel tip (COO^- and NH_3^+ pores). For the PYBA pore, a_B = 139 nm and a_T = 1 nm.

The theoretical results obtained using the above model are shown in Figure 1c and 1d and correspond to the experimental *I–V* curves of Figure 1a and 1b. The nanochannel radii and the surface concentrations of negative ($–COO^-$) and positive ($–NH_3^+$) fixed charge groups before the functionalisation of the UV-sensitive moiety were estimated as follows. Microscopy techniques give the approximate value $a_B = (140 \pm 5)$ nm for the radius of the conical channel base. Introducing this value in the theoretical model gives the fitting parameters a_T = 2 nm and $\sigma = 0.1\ e\ nm^{-2}$ for the radius of the channel tip and the channel surface charge density, respectively (Figure 1a). These values agree with those previously found in similar nanochannels[46] and give theoretical curves (Figure 1c) that can describe the experimental data (Figure 1a) without invoking particular channel shape effects.[13] We use later the same parameters for the charged nanochannel of Figure 1b in the theoretical fitting of Figure 1d. Again, the agreement between the theoretical and experimental curves indicates that the substitution of the original charged groups by the UV-sensitive moieties is almost complete. For the neutralised nanochannel, we obtain a_B = 139 nm, a_T = 1 nm, and $\sigma = 0.1\ e\ nm^{-2}$, which is consistent with the fact that the channel with the attached UV-sensitive moiety should have a lower effective radius than the original channel.

2.2. Multichannel Membranes

UV light-induced changes in the channel surface properties were further investigated by mass transport experiments using a PYBA-modified nanoporous membrane containing an array of cylindrical nanochannels with an aerial density of 5×10^8 channels cm^{-2} with an average diameter of (20 ± 3) nm. Ionic species carrying opposite charge to that of the channel surface will be attracted to and transported selectively through the channel. On the contrary, species with charge of the same sign as that of the surface charge will be repelled and prevented from entering the channel.[47,48] Finally, neutral channels are non-selective, i.e., both cationic and anionic species are almost equally transported across the membrane (**Figure 3**).

For the transport experiments, the PYBA-modified nanoporous membrane was mounted between the two compartments of a conductivity cell and the feed compartment was filled with a 10 mM aqueous solution of methylviologen (MV^{2+})

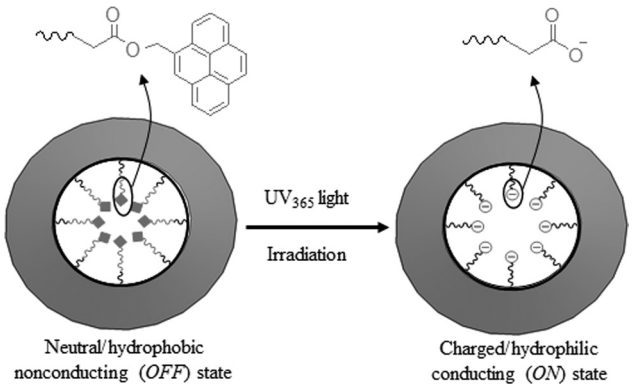

Figure 2. Schematic illustration of the wettability changes produced by UV light irradiation of a single conical nanochannel modified with photoremovable protecting (PYBA) molecules.

or 1,5-naphthalenedisulfonate (NDS^{2-}) prepared in a phosphate buffer (pH = 6.0).

There are three major effects dictating the mass transport through nanochannels: a) volume exclusion, b) hydrophobic, and c) electrostatic interactions. We have studied the transport of the MV^{2+} and NDS^{2-} molecules because of the following reasons: i) they have similar molecular volumes (0.637 and 0.680 nm^3, respectively),[49] ii) the molecular structures of both MV^{2+} and NDS^{2-} contain two benzyl rings giving similar hydrophobic behaviour within the nanochannels, and iii) these molecules have the same charge number in absolute value (they are oppositely charged). Hence, only the surface charges on the inner channel walls dictate the ionic permeation via electrostatic interactions. Because an electrical double layer is formed in the channel, the inside solution has a higher concentration of counter-ions (MV^{2+}) than co-ions (NDS^{2-}).

Figure 3b shows the number of moles for the charged analytes MV^{2+} and NDS^{2-} transported per cm^2 of the PYBA-modified membrane versus time before and after UV light irradiation. The order of magnitude of the MV^{2+} permeation flux (number of moles transported per cm^2 per second) can be estimated from Figure 3b as $J = (8 \times 10^{-9}$ mol $cm^{-2})/6000$ s ~ 10^{-12} mol cm^{-2} s^{-1}. Comparison of this flux with the theoretical estimation $J = \varepsilon Dc/d$ where ε is the porosity, D is the effective diffusion coefficient, c is the feed concentration, and d is the membrane thickness, leads to the effective value $\varepsilon D = 10^{-10}$ cm^2 s^{-1} for $c = 10^{-5}$ mol cm^{-3} and $d = 10^{-3}$ cm.

Before the irradiation, the inner walls of the multichannel membrane are neutral due to the presence of the uncharged photolabile pyrene moieties. These moieties were responsible for the absence of permselective characteristic of the membrane channels as shown in Figure 3a. The permeation of both MV^{2+}

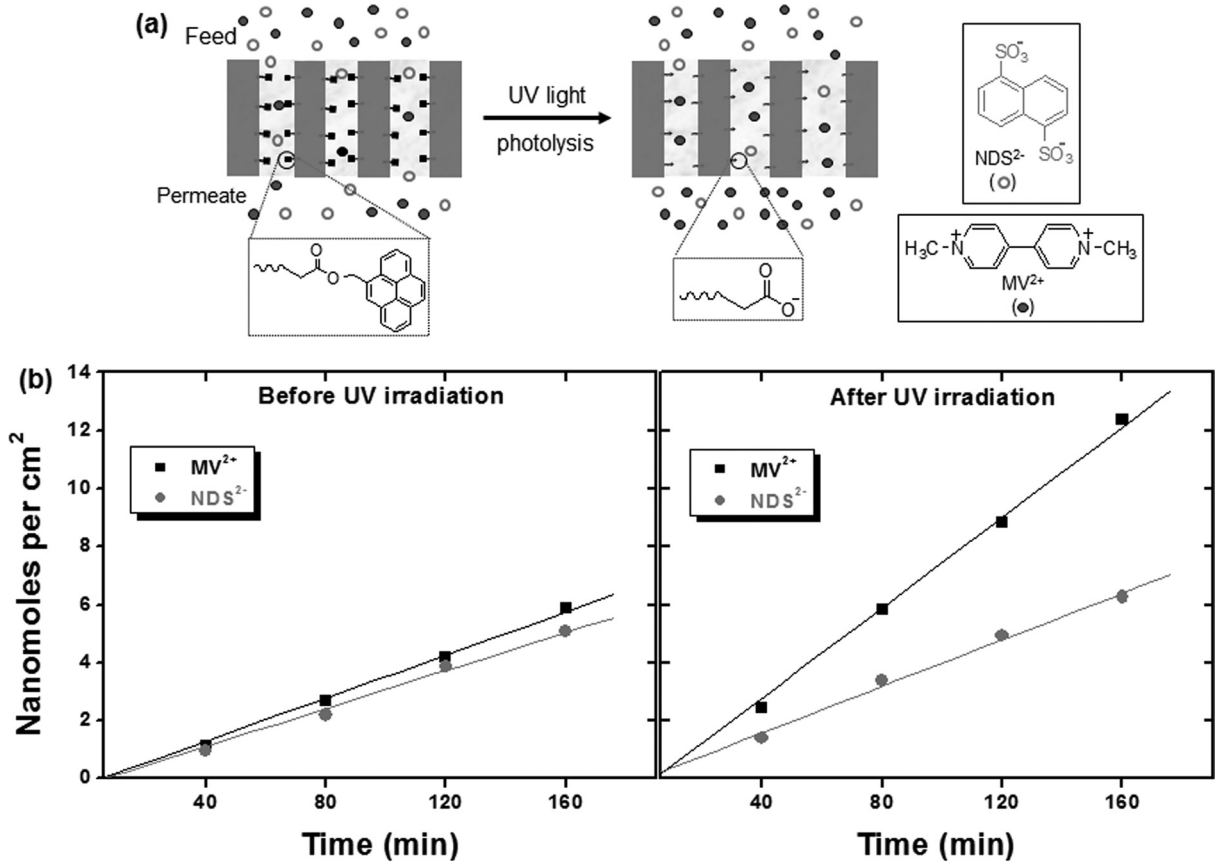

Figure 3. a) Schematic illustration of the transport of ionic species through the multi-channel membrane before and after UV irradiation. b) Permeation data for MV^{2+} and NDS^{2-} prior to and after UV treatment of the PYBA-modified membrane. The fluxes are obtained for an array of cylindrical nanochannels with an average diameter (20 ± 3) nm in a multipore membrane.

and NDS^{2-} molecules is similar despite their opposite charges (see Figure 3b) before the UV treatment. After 160 min of analyte diffusion, 5.9 and 5.1 nanomoles of MV^{2+} and NDS^{2-} were transported through the membrane, respectively. However, these quantities were very different after light irradiation. The permeation of MV^{2+} was remarkably increased with respect to the permeation of NDS^{2-} (see Figure 3b): the light-induced gating led to an increase of ~110% in the number of moles of MV^{2+} transported (from 5.9 to 12.4 nanomoles) while this increase was only of ~23% in the case of NDS^{2-} (from 5.1 to 6.3 nanomoles). Upon UV irradiation of the PYBA-modified channels, the targeted photolabile pyrene moieties were removed leading to exposed carboxylate ($-COO^-$) groups. These moieties transformed the neutral and hydrophobic inner channel walls into the negatively charged and hydrophilic channel walls. Therefore, UV irradiation acted as an optical gating, allowing the PYBA-modified membrane to select the cationic MV^{2+} species over the anionic NDS^{2-} ones. Note finally that we should expect the selectivity of the membranes to change also with the solute size in experiments with other bulky analytes because the pore radius is close to 10 nm.

2.3. Logic Functions and Controlled Release

Logic functions using different combinations of chemical species and electrical potentials as inputs have been proposed.[50] We demonstrated theoretically and experimentally that track-etched single conical nanochannels functionalised with polyprotic acid chains show three levels of conductance that could be tuned externally because of the pH-sensitive fixed charges.[22] Binary and multivalued logical functions were implemented using chemical and electrical inputs.[22] Other logical gate schemes with nanochannels have recently been proposed.[16,51,52] Potential applications of nanofluidics-based logical functions involve information processing, sensing, and controlled release of chemicals in liquid media. In particular, integration of microchannels and nanochannels in chip-based ionic circuits[53,54] should be useful for analytical and pharmaceutical applications.

Light-based molecular systems for information processing typically use chemical signals as inputs and optical (e.g., fluorescence) signals as outputs.[55–57] Alternatively, the light-gated nanochannel studied here could be used to implement a variety of logic functions using optical and electrical signal as the inputs and electrical and chemical signals as the outputs. Some examples are given in **Table 1**, **2**, and **3**, where the multichannel membrane selectivity was quantified by the ratio of ionic fluxes $S = (J_{MV^{2+}} - J_{NDS^{2-}}) / (J_{MV^{2+}} + J_{NDS^{2-}})$. From the experimental data of Figure 3b, $S = 0.067$ before the UV irradiation and $S = 0.320$ after irradiation. Future implementation of reset functions could be achieved by light-induced conformational changes in the functionalised molecules, thus avoiding the irreversible molecular detaching employed here.

Irreversibility phenomena and accumulation of chemical waste could be serious problems for chemically driven molecular logic devices. While in our case the reset function could be provided by light-induced conformational changes in the functionalised molecules,[58,59] the fact is that for controlled release applications based on the optical gating of the multichannel membrane (see Figure 3), the irreversibility should not be a serious issue because the chemical drug is intended to be absorbed by the external solution after release.

Table 1. YES logic function for the single nanochannel with an optical input and an electrical output.

Input	Output
UV light	I(nA) at $V = +2$ V
Off (0)	0.11 (0)
On (1)	0.84 (1)

Table 2. YES logic function for the multichannel membrane with an optical input and a chemical output.

Input	Output
UV light	Ionic selectivity S
Off (0)	0.07 (0)
On (1)	0.32 (1)

Table 3. AND logic function for the single nanochannel with electro-optical inputs and an electrical output.

Input		Output
V (V)	UV light	G (nS)
–2 (0)	Off (0)	0.03 (0)
–2 (0)	On (1)	0.05 (0)
2 (1)	Off (0)	0.06 (0)
2 (1)	On (1)	0.42 (1)

3. Conclusion

We used 4-oxo-4-(pyren-4-ylmethoxy) butanoic acid as the photolabile protecting group to design a light-gated nanofluidic device based on synthetic ion channels. The inner walls of the channels were decorated with monolayers of photolabile molecules that can be removed by irradiation with UV light. This process leads to the generation of hydrophilic groups and the concomitant permselective transport of the ionic species in aqueous solution through the channels. In particular, we characterised experimentally and theoretically the optical gating of a conical nanochannel and a multichannel polymeric membrane by means of current–voltage and selective permeation measurements. We anticipate that the integration of nanostructures into multifunctional devices is feasible, and should readily find applications in light-induced controlled release, sensing, and information processing. In particular, the nanofluidic devices should allow different optical, chemical and electrical signals to be used as inputs and outputs.

4. Experimental Section

Materials: Methylviologen dichloride (MV^{2+}), 1,5-naphthalene disulfonate di-sodium salt (NDS^{2-}), *N*-(3-dimethylaminopropyl)-*N*′-ethylcarbodiimide hydrochloride (EDC), pentafluorophenol (PFP),

ethylenediamine (EDA), 1-pyrenemethanol (Py) and succinic anhydride were purchased from Sigma–Aldrich, Germany. All the reagents were of analytical grade and used as received without further purification.

Polyethylene terephthalate (PET) membranes of 12 μm thickness (Hostaphan RN 12, Hoechst) were irradiated at the linear accelerator UNILAC (GSI, Darmstadt) with swift heavy ions (Pb, U or Au) with energy of 11.4 MeV per nucleon.

Fabrication of Nanochannels: In order to improve etching of latent tracks, heavy ion irradiated PET membranes were first sensitised with UV light for 15 minutes from each side. The UV source provided a light intensity of 30 W m^{-2} with a maximum wavelength at 320 nm.

Single Conical Nanochannels Fabrication: PET membranes with single ion track were used for the fabrication of single conical nanochannels via an asymmetric track-etching technique developed by Apel and co-workers.[10] Briefly, the heavy ion tracked membrane was mounted between the two compartments of a conductivity cell. The membrane acted as a dividing wall between the compartments. The etching process was carried out at room temperature. In one compartment of the cell, an etching solution (9 M NaOH) was filled while a stopping solution (1 M HCOOH + 1 M KCl) was added in the other compartment. In order to monitor the track-etching process, a potential of –1 V was applied across the membrane and the current was monitored continuously across the membrane via a picoammeter/voltage source (Keithley 6487, Keithley Instruments, Cleveland, OH). The etchant slowly etched the latent track and the current remained zero until the etchant penetrated through the whole length of the membrane. At this moment, a sudden increase in the current marked the breakthrough point. After the breakthrough, permeated etchant was immediately neutralised by the stopping solution placed on the other side of the membrane. The etching process was terminated when the current reached a value of 0.1 nA approximately. Subsequently, the etched membranes were washed with stopping solution in order to quench the etchant and immersed in deionised water overnight in order to remove the residual salts.

The base diameter of the conical channel was determined from the multichannel membrane (etched along with the single-channel membrane) by field-emission scanning electron microscopy (FESEM). The tip diameter of single conical channel could be estimated from the fitting of the *I–V* curve measured at pH = 3 in a 1 M KCl electrolyte solution. Under these conditions the *I–V* curve is linear and the only fitting parameter in the theoretical model is a_R.

Preparation of Cylindrical Nanochannel Array: For this purpose, PET membranes irradiated with 5×10^8 ions cm^{-2} were used. The fabrication of cylindrical nanochannels was achieved by the symmetric track-etching technique.[60] Polymer membranes fixed in a sample holder were immersed in the pre-heated etching solution. During the whole etching process, the etching solution was continuously stirred in order to provide a homogeneous etchant concentration in the bath and the temperature was maintained at 50 °C by circulating heated water through the double walls of the beaker. After etching, the membranes were taken out from the solution and rinsed several times with distilled water. For further removal of the residual salts, the etched membranes were additionally immersed in deionised water overnight.

Synthesis of 4-oxo-4-(pyren-4-ylmethoxy) butanoic acid (PYBA): The synthesis of PYBA was carried out following a previously reported method.[37] 1-pyrenemethanol (2.15 mmol, 500 mg) was added to a solution of succinic anhydride (2.80 mmol, 280 mg) in dichloromethane (80 mL). After complete dissolution of 1- pyrenemethanol, pyridine (266.6 mmol, 21.5 mL) was added into the solution dropwise. The reaction mixture was stirred at 50 °C for 18 h and a 30% (*v*/*v*) aqueous solution of hydrochloric acid (100 mL) was added to remove excess of pyridine. The reaction mixture was then extracted three times with dichloromethane (50 mL). The combined organic layers were collected, washed three times with water (50 mL), and dried over anhydrous sodium sulfate. After filtration, the solvent was evaporated under reduced pressure to afford 4-oxo-4-(pyren-4-ylmethoxy) butanoic acid (PYBA) as a light yellow powder (465 mg, 65%). ^{1}H-NMR (200 MHz, $CDCl_3$): δ = 8.17–7.88 (m, 9H, H-arom), 5.77 (s, 2H, $-CH_2-$), 2.59 (s, 4H, $-CH_2CH_2-$).

Functionalisation of Nanochannels: The covalent immobilisation of photolabile protecting molecules onto the channel surface was accomplished in two steps. Firstly, the carboxyl groups on the channel surface were converted into amine reactive PFP-esters by immersing the track-etched membranes in an ethanolic solution containing a mixture of *N*-(3-dimethylaminopropyl)-*N′*-ethylcarbodiimide hydrochloride (EDC, 100 mM) and pentafluorophenol (PFP, 200 mM). The activation process was carried out for one hour. After washing with ethanol, the activated membranes were treated with a ethylenediamine (EDA, 50 mM) solution prepared in ethanol for the amination of channel surface. Subsequently, the aminated membranes were washed first with ethanol and finally with deionised water. Secondly, the aminated membranes were exposed to a solution of 4-oxo-4-(pyren-4-ylmethoxy) butanoic acid (PYBA, 10 mM) along with an activating agent (EDC, 50 mM) in ethanol. In this step, the amine groups on the channels surface were allowed to covalently couple with the carboxyl group of PYBA in a reaction carried out for two hours. Finally, the modified membranes were thoroughly washed with ethanol.

It should be cited that alternative photoremovable groups have been studied previously for protecting carboxylic acids. In particular, benzyl, nitrophenyl and nitobenzyl groups were employed successfully for the surface modification of different materials in order to tune their wettability upon UV irradiation. However, the fact is that some of the photolabile groups behave differently when we switched from surface to nanoconfined geometries. Moreover, our choice of pyrene is based on the previous studies,[38] which demonstrated that, after UV irradiation, the recovery of carboxylic acid moieties is maximum when they are protected with pyrenemethyl esters groups in mild conditions.[27]

UV Light Irradiation: The PYBA-modifies membranes were irradiated with UV light of wavelength 365 nm for 10 min on each side in dry state. For UV light irradiation, an Oriel Instruments 500 W mercury lamp was used with a 365 nm filter. After irradiation, membranes were washed first with ethanol followed by deionised water in order to remove the photocleaved groups from the interior of the nanochannels.

Following a previous study,[38] we selected a minimum exposition time of 10 min on each side of the polymeric membrane containing the nanochannels. This time is enough to remove most of the photolabile moieties from the channel surface, as confirmed by the subsequent transport experiments. The successful cleavage of pyrene moieties was further confirmed by the *I–V* curves in the case of the single nanopore.

Current–Voltage Measurements: The membrane with a single channel was characterised by measuring the *I–V* curves. To this end, a single-channel membrane was mounted between the two halves of the conductivity cell. An electrolyte solution (0.1 M KCl, pH 6.0) was filled on both sides of the membrane. An Ag/AgCl electrode was placed into each half-cell solution and the ionic current flowing through the single channel membrane was measured with a picoammeter/voltage source (Keithley 6487, Keithley Instruments, Cleveland, OH). The ground electrode was placed on the base opening side of the conical nanochannel and the *I–V* curves were recorded by applying a scanning triangle voltage signal from –2 to +2 V across the membrane.

Transport Experiments: The multichannel membrane was placed between the two halves of the conductivity cell. Each cell volume was 3.4 mL with an effective membrane permeation area of 1.15 cm^2. The feed half-cell contained a known concentration (10 mM) of each organic analyte [methyl viologen (MV^{2+}) and 1,5-naphthalenedisulfonic acid (NDS^{2-})] prepared in the buffer solution. The permeate half-cell was filled with a pure buffer solution. Both solutions were continuously stirred during the experiment. After fixed time periods, the concentrations of respective analytes in the permeate half-cell were estimated from the UV absorbance values. Similar transport experiments were performed after UV_{365} light irradiation of the PYBA-modified membrane.

Acknowledgements

M.A., S.N., Q.H.N., and W.E. gratefully acknowledge financial support by the Beilstein-Institut, Frankfurt/Main, Germany, within the research collaboration NanoBiC. P.R. and S.M. acknowledge the financial support from the Ministry of Science and Innovation of Spain, Programme of

Materials (project No. MAT2009-07747), and FEDER. I.A. and L.F. were financially supported by KIT Excellence Initiative, project A5.7. The authors thank Dr. Christina Trautmann from GSI (Department of Materials Research) for support with the heavy ion irradiation experiments. We also acknowledge Dr. Muhammad Nawaz Tahir (Mainz University) for fruitful discussions and help in performing the UV light irradiation experiments.

Received: September 9, 2011
Published online: November 8, 2011

[1] E. Gouaux, R. MacKinnon, *Science* **2005**, *310*, 1461.
[2] J. Griffiths, *Anal. Chem.* **2008**, *80*, 23.
[3] B. Hille, *Ionic channels of excitable membranes*, Sinauer Associates Inc., Sunderland, MA **2001**.
[4] H. Bayley, P. S. Cremer, *Nature* **2001**, *413*, 226.
[5] C. Dekker, *Nat. Nanotechnol.* **2007**, *2*, 209.
[6] X. Hou, W. Guo, L. Jiang, *Chem. Soc. Rev.* **2011**, *40*, 2385.
[7] R. Karnik, C. H. Duan, K. Castelino, H. Daiguji, A. Majumdar, *Nano Lett.* **2007**, *7*, 547.
[8] Z. S. Siwy, *Adv. Funct. Mater.* **2006**, *16*, 735.
[9] H. S. White, A. Bund, *Langmuir* **2008**, *24*, 2212.
[10] P. Y. Apel, Y. E. Korchev, Z. Siwy, R. Spohr, M. Yoshida, *Nucl. Instrum. Methods Phys. Res., Sect. B* **2001**, *184*, 337.
[11] J. Cervera, B. Schiedt, R. Neumann, S. Mafe, P. Ramirez, *J. Chem. Phys.* **2006**, *124*, 104706.
[12] J. Cervera, B. Schiedt, P. Ramirez, *Europhys. Lett.* **2005**, *71*, 35.
[13] P. Ramirez, P. Y. Apel, J. Cervera, S. Mafe, *Nanotechnology* **2008**, *19*, 315707.
[14] M. R. Powell, M. Sullivan, I. Vlassiouk, D. Constantin, O. Sudre, C. C. Martens, R. S. Eisenberg, Z. S. Siwy, *Nat. Nanotechnol.* **2008**, *3*, 51.
[15] a) M. Ali, R. Neumann, W. Ensinger, *ACS Nano* **2010**, *4*, 7267; b) M. Ali, Q. H. Nguyen, R. Neumann, W. Ensinger, *Chem. Commun.* **2010**, *46*, 6690.
[16] a) M. Ali, P. Ramirez, M. N. Tahir, S. Mafe, Z. Siwy, R. Neumann, W. Tremel, W. Ensinger, *Nanoscale* **2011**, *3*, 1894; b) M. Ali, M. N. Tahir, Z. Siwy, R. Neumann, W. Tremel, W. Ensinger, *Anal. Chem.* **2011**, *83*, 1673.
[17] I. Vlassiouk, T. R. Kozel, Z. S. Siwy, *J. Am. Chem. Soc.* **2009**, *131*, 8211.
[18] M. Ali, B. Schiedt, R. Neumann, W. Ensinger, *Macromol. Biosci.* **2010**, *10*, 28.
[19] G. L. Wang, A. K. Bohaty, I. Zharov, H. S. White, *J. Am. Chem. Soc.* **2006**, *128*, 13553.
[20] A. Kocer, M. Walko, W. Meijberg, B. L. Feringa, *Science* **2005**, *309*, 755.
[21] A. Alcaraz, P. Ramirez, E. Garcia-Gimenez, M. L. Lopez, A. Andrio, V. M. Aguilella, *J. Phys. Chem. B* **2006**, *110*, 21205.
[22] M. Ali, S. Mafe, P. Ramirez, R. Neumann, W. Ensinger, *Langmuir* **2009**, *25*, 11993.
[23] M. Ali, P. Ramirez, S. Mafe, R. Neumann, W. Ensinger, *ACS Nano* **2009**, *3*, 603.
[24] B. Yameen, M. Ali, R. Neumann, W. Ensinger, W. Knoll, O. Azzaroni, *Small* **2009**, *5*, 1287.
[25] X. Hou, F. Yang, L. Li, Y. L. Song, L. Jiang, D. B. Zhu, *J. Am. Chem. Soc.* **2010**, *132*, 11736.
[26] C. G. Bochet, *J. Chem. Soc., Perkin Trans. 1* **2002**, 125.
[27] M. Iwamura, T. Ishikawa, Y. Koyama, K. Sakuma, H. Iwamura, *Tetrahedron Lett.* **1987**, *28*, 679.
[28] A. Patchornik, B. Amit, R. B. Woodward, *J. Am. Chem. Soc.* **1970**, *92*, 6333.
[29] A. P. Pelliccioli, J. Wirz, *Photochem. Photobiolog. Sci.* **2002**, *1*, 441.
[30] R. Reinhard, B. F. Schmidt, *J. Org. Chem.* **1998**, *63*, 2434.
[31] U. Zehavi, B. Amit, A. Patchornik, *J. Org. Chem.* **1972**, *37*, 2281.
[32] *Dynamic Studies in Biology: Phototriggers, Photoswitches and Caged Biomolecules*, (Eds: M. Goeldner, R. Givens), Wiley-VCH, Weinheim, Germany **2005**.
[33] S. P. A. Fodor, J. L. Read, M. C. Pirrung, L. Stryer, A. T. Lu, D. Solas, *Science* **1991**, *251*, 767.
[34] D. Orain, J. Ellard, M. Bradley, *J. Comb. Chem.* **2002**, *4*, 1.
[35] A. A. Brown, O. Azzaroni, W. T. S. Huck, *Langmuir* **2009**, *25*, 1744.
[36] K. Critchley, J. P. Jeyadevan, H. Fukushima, M. Ishida, T. Shimoda, R. J. Bushby, S. D. Evans, *Langmuir* **2005**, *21*, 4554.
[37] W. Cui, X. M. Lu, K. Cui, J. Wu, Y. Wei, Q. H. Lu, *Nanotechnology* **2011**, *22*.
[38] J. Q. Jiang, X. Tong, Y. Zhao, *J. Am. Chem. Soc.* **2005**, *127*, 8290.
[39] J. P. Lai, X. Mu, Y. Y. Xu, X. L. Wu, C. L. Wu, C. Li, J. B. Chen, Y. B. Zhao, *Chem. Commun.* **2010**, *46*, 7370.
[40] B. Zhao, J. S. Moore, D. J. Beebe, *Science* **2001**, *291*, 1023.
[41] Z. Siwy, P. Apel, D. Dobrev, R. Neumann, R. Spohr, C. Trautmann, K. Voss, *Nucl. Instrum. Methods Phys. Res., Sect. B* **2003**, *208*, 143.
[42] M. Ali, B. Schiedt, K. Healy, R. Neumann, W. Ensinger, *Nanotechnology* **2008**, *19*, 085713.
[43] M. Ali, B. Yameen, R. Neumann, W. Ensinger, W. Knoll, O. Azzaroni, *J. Am. Chem. Soc.* **2008**, *130*, 16351.
[44] L. E. Ermakova, M. P. Sidorova, M. E. Bezrukova, *Colloid J.* **1998**, *52*, 705.
[45] M. Ali, V. Bayer, B. Schiedt, R. Neumann, W. Ensinger, *Nanotechnology* **2008**, *19*, 485711.
[46] M. Ali, B. Yameen, J. Cervera, P. Ramirez, R. Neumann, W. Ensinger, W. Knoll, O. Azzaroni, *J. Am. Chem. Soc.* **2010**, *132*, 8338.
[47] C. R. Martin, M. Nishizawa, K. Jirage, M. S. Kang, S. B. Lee, *Adv. Mater.* **2001**, *13*, 1351.
[48] M. Nishizawa, V. P. Menon, C. R. Martin, *Science* **1995**, *268*, 700.
[49] S. B. Lee, C. R. Martin, *Anal. Chem.* **2001**, *73*, 768.
[50] M. Pita, E. Katz, *J. Am. Chem. Soc.* **2008**, *130*, 36.
[51] J. Cervera, P. Ramirez, S. Mafe, P. Stroeve, *Electrochim. Acta* **2011**, *56*, 4504.
[52] S. Mafe, J. A. Manzanares, P. Ramirez, *J. Phys. Chem. C* **2010**, *114*, 21287.
[53] J. H. Han, K. B. Kim, H. C. Kim, T. D. Chung, *Angew. Chem. Int. Ed.* **2009**, *48*, 3830.
[54] W. Zhan, R. M. Crooks, *J. Am. Chem. Soc.* **2003**, *125*, 9934.
[55] A. P. de Silva, I. M. Dixon, H. Q. N. Gunaratne, T. Gunnlaugsson, P. R. S. Maxwell, T. E. Rice, *J. Am. Chem. Soc.* **1999**, *121*, 1393.
[56] P. Remon, R. Ferreira, J. M. Montenegro, R. Suau, E. Perez-Inestrosa, U. Pischel, *ChemPhysChem* **2009**, *10*, 2004.
[57] G. Q. Zong, G. X. Lu, *J. Phys. Chem. C* **2009**, *113*, 2541.
[58] K. Smaali, S. Lenfant, S. Karpe, M. Ocafrain, P. Blanchard, D. Deresmes,S. Godey, A. Rochefort, J. Roncali, D. Vuillaume, *ACS Nano* **2010**, *4*, 2411.
[59] G. Pace, V. Ferri, C. Grave, M. Elbing, C. von Hanisch, M. Zharnikov, M. Mayor, M. A. Rampi, P. Samori, *Proc. Nat. Acad. Sci. USA* **2007**, *104*, 9937.
[60] Q. H. Nguyen, M. Ali, V. Bayer, R. Neumann, W. Ensinger, *Nanotechnology* **2010**, *21*, 365701.